HHS Public Access

Author manuscript

Cancer Res. Author manuscript; available in PMC 2017 March 15.

Published in final edited form as:

Cancer Res. 2016 September 15; 76(18): 5383–5394. doi:10.1158/0008-5472.CAN-15-3159.

The NSL chromatin-modifying complex subunit KANSL2 regulates cancer stem-like properties in glioblastoma that contribute to tumorigenesis

Nazarena Ferreyra-Solari[1], **Fiorella S. Belforte**[1], **Lucía Canedo**[1], **Guillermo A. Videla-Richardson**[2], **Joaquín M. Espinosa**[3], **Mario Rossi**[1], **Eva Serna**[4], **Miguel A. Riudavets**[5,6], **Horacio Martinetto**[5], **Gustavo Sevlever**[5], and **Carolina Perez-Castro**[1,*]

[1]Instituto de Investigación en Biomedicina de Buenos Aires (IBioBA) - CONICET- Partner Institute of the Max Planck Society. Buenos Aires, Argentina

[2]Laboratorio de Investigación aplicada a Neurociencias (LIAN). Fundación para la Lucha contra las Enfermedades Neurológicas de la Infancia (FLENI). Ruta 9, Km 52.5, B1625XAF. Escobar. Buenos Aires, Argentina

[3]Linda Crnic Institute for Down Syndrome, Department of Pharmacology, University of Colorado School of Medicine, Aurora, Colorado, U.S.A

[4]Servicio Análisis Multigénico. Unidad Central de Investigación. Facultad de Medicina. Universidad de Valencia. España

[5]Laboratorio de Biología Molecular, Departamento de Neuropatología y Biología Molecular. Fundación para la Lucha contra las Enfermedades Neurológicas de la Infancia (FLENI). Montañeses 2325, C1428AQK. Buenos Aires, Argentina

[6]Laboratorio de Histopatología. Cuerpo Médico Forense. Tribunal Supremo de Justicia. Buenos Aires, Argentina

Abstract

KANSL2 is an integral subunit of the Non-Specific Lethal (NSL) chromatin-modifying complex which contributes to epigenetic programs in embryonic stem cells. In this study, we report a role for KANSL2 in regulation of stemness in glioblastoma (GBM), which is characterized by heterogeneous tumor stem-like cells associated with therapy resistance and disease relapse. KANSL2 expression is upregulated in cancer cells, mainly at perivascular regions of tumors. RNAi-mediated silencing of KANSL2 in GBM cells impairs their tumorigenic capacity in mouse xenograft models. In clinical specimens, we found that expression levels of KANSL2 correlate with stemness markers in GBM stem-like cell populations. Mechanistic investigations showed that KANSL2 regulates cell self-renewal, which correlates with effects on expression of the stemness transcription factor POU5F1. RNAi-mediated silencing of POU5F1 reduced KANSL2 levels, linking these two genes to stemness control in GBM cells. Together, our findings indicate that

Corresponding Author: Carolina Perez-Castro Ph.D., Instituto de Investigación en Biomedicina de Buenos Aires (IBioBA) - CONICET- Partner, Institute of the Max Planck Society, Polo Científico Tecnológico. Godoy Cruz 2390, C1425FQD, Buenos Aires, Argentina, Teléfono (+5411) 4899-5500., cperezcastro@ibioba-mpsp-conicet.gov.ar.

Disclosure of Potential Conflicts of Interest: No potential conflicts of interest were disclosed.

KANSL2 acts to regulate the stem cell population in GBM, defining it as a candidate GBM biomarker for clinical use.

Keywords

KANSL2; tumorigenesis; POU5F1; glioblastoma; *stemness*

INTRODUCTION

Glioblastoma (GBM) is among the most frequent, aggressive and lethal tumor types within the central nervous system (CNS) (1,2) and for which there is no effective treatment. Thus, identification of critical signaling pathways involved in GBM progression may enable the development of new diagnostic and therapeutic strategies. GBM stem cells (GBSCs) are small neoplastic cell populations with the ability to self-renew and eventually differentiate to glial and neural cell types (3–5). GBSCs have enhanced tumor initiation capacity and are able to regenerate the heterogeneous cell population observed in GBM, contributing to tumor maintenance and recurrence after treatment (6).

Many of the key signaling pathways involved in embryonic stem cells (ESC) identity, including core pluripotency factors and epigenetic regulators, are also functional in GBSCs (7–10). Expression of POU5F1 (Oct4), an ESC factor, is critical for their *stemness in vitro* and tumorigenicity *in vivo* (11–14). In accordance, GBSCs can grow as multipotent clonal spheres, called gliomaspheres, which exhibit most of the biological and pathological characteristics of cancer stem cells (CSC) (3,6,15). We hypothesized that *stemness* genes are involved in dysregulation of cell plasticity events in GBM. We performed an *in silico* search to mine publicly available mRNA expression and ChIP-seq data (16–19) using the web tool INSECT (In silico search for co-occurring transcription factors) (20), to identify genes that are commonly expressed both in pluripotent stem cells and CSCs, exhibiting potential binding sites for POU5F1 in their regulatory region. Using this approach, we identified *KANSL2* (KAT8 regulatory NSL complex subunit 2) as a strong candidate gene. The KANSL protein family belongs to the lysine acetyl-transferase KAT8/MOF-NSL complex and its function has been linked to pluripotency and cellular homeostasis in ESCs (21–23). KANSL2 is a poorly understood member of the NSL complex family and its role has not been previously explored in glioblastoma.

Here, we characterized the role of KANSL2 in GBM cells. KANSL2 is up-regulated in glioma samples and expressed mainly in perivascular regions and in discrete foci within tissues. *KANSL2* upregulation was also observed in patient-derived GBM cell lines showing stem cell features with increased *POU5F1*, *NANOG*, *NESTIN* and *CD133* expression. Importantly, we determined that KANSL2 expression is critical for stem cell properties of GBM cells, as *KANSL2* depletion reduced neurosphere formation, *POU5F1* expression and tumorigenesis. Moreover, KANSL2 and *POU5F1* enforce expression of each other, making a regulatory feedback loop that might control *stemness* properties in this cancer type.

MATERIALS AND METHODS

Unless otherwise stated, reagents were obtained from Life Technologies or Sigma Chemical Co.

Tissue samples

Samples obtained from the tumor bank at FLENI Hospital, were subjected to histological diagnosis by experienced neuropathologists and collected with informed consent according to the hospital's institutional review board (in compliance with the October 2013 Helsinki Declaration). Patient and tumor sample information is listed in Table 1.

Microarray analysis was performed on a cohort containing 52 gliomas specimens as described (24) (Accession Number: E-MTAB-4455) (Supplementary Table S1). Fisher's exact test was used for statistical analysis of gene expression, cut-off p-value ≤ 0.05 (24).

IHC staining and analyses

Biopsies were conducted as previously described (25). For Immunohistochemistry staining with Leica Bond Max automated Stainer, the following antibodies were used: anti-KANSL2 (Sigma-Aldrich HPA038497, specificity confirmed by shRNA-mediated knockdown); anti-KAT8 (Santa Cruz Biotechnology INC sc-271691) and anti-AcH4K16 (Abcam ab109463) (Table 1) (26,27). Images were acquired with a NikonDXN1200F digital camera controlled by EclipseNet software (version1.20.0 build 61). Unbiased stereological analysis was also used to quantify anti-KANSL2- and anti-Ki-67- (NCL-Ki67-MM1 Novocastra Laboratories) labeled elements in tumor samples using Stereo Investigator Optical Dissector software (MBF Biosciences, MicroBrightField, Inc). Necrotic areas were also examined (additional experimental information).

Cell Culture

Patient-derived stem cells, G03 and G08, were established from human GBM grade IV biopsies, identify and characterized previously (25). Briefly, cells with the same genomic alterations as parental tumors were cultured in neural stem cell (NSC) medium plus supplements (25) and plated onto laminin-coated plates. Their cellular hierarchy and plasticity (markers expression, differentiation and tumorigenic potential) were previously characterized (25). Cell lines U87MG, T98G, LN299, HEK293T, C6, P19 and WA09 (H9) were acquired from ATCC or WiCell Research Institute, either directly or by colleagues, kept frozen immediately after receipt or used in culture less than 4 months. ATCC cell lines were characterized by Short Tandem Repeat (STR) profiling and WiCell lines by testing established standards for ECSs culture and G-band karyotype. For neurosphere induction, GBM cells were grown to 90% confluence, trypsinized, and plated in neural stem cell (NSC) medium in ultra-low adhesion multi-well plates (Corning). After 5 days, the number of spheres was quantified using 10× magnifications under a phase contrast microscope (Carl-Zeiss, AxioObserverZ1), an AxioCam(HRm) camera (Carl-Zeiss) and Zen pro2011; and later collected for RNA analysis. For *in vitro* propagation, spheres were collected by gentle centrifugation, dissociated to single cells, and cultured to produce the next generation of spheres.

KANSL2-RFP construct

cDNA encoding the murine KANSL2 (Gene ID: 69612) was amplified from pluripotent P19 embryonal carcinoma cells with the specific primers. Forward 5-GACCATGAACAGGATTCGGA-3 and Reverse 5-ACCGGTGGACTGATAGAAGTGGG-3, containing EcoRI and AGE I sites for cloning into pGEMT vector (Promega). Insert was subcloned into pTagRFP-N (Evrogen) to generate KANSL2-RFP.

Flow Cytometry and Cell Sorting Analysis

Cells were incubated with anti-CD133/1 (AC133)-PE conjugate antibody (130-080-801) (Miltenyi Biotec) (25). Data was acquired on a FACSCantoII instrument (BD Biosciences) and analyzed using FlowJo software version10. The isotype control sample was used to establish a gate in the PE channel. Cells showing signal for CD133 above the gate established were deemed to be CD-positive cells. Jazz Cell Sorter (BD Biosciences) was used for the analysis under the settings of “1.5 Drop Pure” from “FACS Software”.

Quantitative Real-time PCR

Total RNA was extracted by Trizol following manufacturer’s instructions. cDNA was synthesized using MMLV reverse transcriptase (Promega). Real-time PCR was performed using Bio-Rad CFX96 Touch™ Real-Time PCR Detection System and a Real Supermix Kit (Bio-Rad). RPL19 or GAPDH were used as normalization controls. Relative expression was calculated with the $2^{-\Delta\Delta CT}$ method (28). Averages of three independent experiments ± SEM are shown. Primers are listed in Supplementary Table S2.

shRNA knockdown

Knockdown cell lines were generated using Sigma Mission shRNA lentiviral plasmids. Lentiviral particles were produced in HEK293T cells by cotransfection of the shRNA vector and lentiviral helper plasmids. To establish stable cell lines, monolayers of different GBM cell lines were subjected to 2 rounds of infection. Stable control and specific knockdown pools were selected and maintained with puromycin (2.5μg/ml). Mission pLKO.5-puro Non-Target shRNA plasmid (#SHC202) was used as a control. Knockdown efficiency was confirmed by qRT-PCR and western blotting. Target sequences are listed in Supplementary Table S3.

Luciferase assays

HEK293 cells (3×10^5cells/well) were seeded onto 12-well plates and co-transfected with Lipofectamine2000 with pKANSL2-RFP, pLM-vexGFP-Oct4 (a gift from Michel Sadelain, Addgene plasmid #22240), B-galactosidase (RSV b-galactosidase), phOCT4 (a gift from Shinya Yamanaka, Addgene plasmid #17221), or pNANOG-Luc (a gift from Ren-he Xu, Addgene plasmid #25900) (500:250:500ng respectively). After 24h, cells were lysed and luciferase and B-galactosidase (B-Gal) activities measured (Promega). To calculate transcriptional activity, each value was normalized to that of B-Gal, and expressed by the mean ± SEM.

Western Blotting

Cells were lysed in radioimmunoprecipitation assay buffer (RIPA) with 1% Triton X-100 and a protease inhibitor cocktail (Roche, USA). Protein samples were separated by SDS-PAGE, blotted onto Immobilon-P PVDF membrane (Millipore) and probed with antibody. Primary antibodies specific to KANSL2 (Sigma-Aldrich, HPA038497), KAT8 (Santa Cruz Biotechnology, INC, sc-271691), AcH4K16 (Abcam, ab109463), H3 (Cell Signaling), POU5F1 (Abcam, ab19857), and GAPDH (Abcam, ab8245) were used. Blots were incubated with goat anti-rabbit or anti-mouse secondary antibody (BioRad Life Science) and visualized using ECL (Supersignal, Thermo Fisher Scientific).

Cell Proliferation

All cultures were passaged by mechanical dissociation of spheres and seeded in quadruplicate into 96 wells at a density of 2×10^3 cells/well. After 72 h cell growth was measured by direct counting or with the MTT-based CellTiter96 Aqueous One Solution Cell Proliferation Assay Kit (Promega).

Limiting Dilution Assay

Cells were dissociated and plated at 1, 10, 25, 50, 100 and 200 cells/well in NSC medium into a 96-well plate. Between 5 to 7 days after plating, the number of neurospheres found in each well was quantified under the microscope. Tumor-initiating cell (TIC) frequency and p-values were calculated using ELDA software (29).

Soft agar colony formation assay

1×10^4 U87MG cells were plated in soft agar, each well contained 2 ml of 0.6% agar and NSC medium 2X and then, covered with 2 ml of 0.3% agar and NSC medium. Fresh NSC medium was added twice a week. After 3 weeks, wells were fixed with 4% paraformaldehyde and stained with 0.005% crystal violet.

Mouse xenograft model

NOD*scid* mice (Jackson Laboratory) of 6–8 weeks of age according to NIH guidelines were injected subcutaneously on the right dorsum (~5 mice/group) with 2×10^6 U87MG cells or 1×10^6 LN229 cells. For intracranial tumor development, cells were stereotaxically injected (0.7–1 mm posterior, 2 mm left lateral, 3.5 mm in depth from the dura) (30). Survival was assessed by Kaplan-Meier analysis and long-rank testing.

Statistical analyses

Data was analyzed using Prism GraphPAD v6.0, and presented as the mean ± SEM from three independent experiments. Two-tailed Student's t-tests and one-way ANOVA were used to define statistical significance *$p\leq0.05$, **$p\leq0.005$, and ***$p\leq0.0005$. Progenitor frequencies from limiting dilution assays were determined using the software tool (ELDA) (29).

RESULTS

KANSL2 is overexpressed in human glioblastoma samples

In order to identify novel genes expressed in stem cells and potentially regulated by POU5F1 in human and mouse, we employed the bioinformatics tool INSECT (20). Among the top scoring genes, we found *KANSL2* as a potential candidate (Supplementary Fig. S1A, B, C and D). KANSL2 (previously known as C12orf41) is a member of the NSL complex expressed in ESCs (31–34), also reported to be up-regulated in Ntera-2 human pluripotent embryonic carcinoma cells. This cell line shows ESC features and is considered to be a malignant counterpart of human embryonic cells (18,19,35,36). We first confirmed by qRT-PCR that *KANSL2* is indeed expressed in embryonic and carcinoma stem cells and its expression is reduced during differentiation to embryoid bodies (EBs) (Supplementary Fig. S1E and F). It has been reported that GBSCs display neural stem/progenitor cells (NSC) properties (37,38). We determined that *KANSL2* is expressed in human neuronal progenitors (NPs) (Supplementary Fig. S1E). Next, we analyzed *KANSL2* expression in high-grade glioma samples and normal human cortex by qRT-PCR, observing *KANSL2* expression significantly enriched in tumor samples (~7 fold) (Figure 1A). *POU5F1* mRNA was also highly expressed in the same human tissue samples (Figure 1A) (12,13).

To further evaluate *KANSL2* expression in GBM samples, we analyzed KANSL2 protein distribution and accumulation by immunohistochemical staining (IHC). All tumor samples were tested in duplicate and individual sections were scored and quantified (Table 1). We did not observe signal for KANSL2 expression in any of the normal tissues examined (8/8 cases). In contrast, tumor samples displayed consistently high KANSL2 expression (7/7) (Figure 1B and Table 1). Interestingly, we detected very visible KANSL2 protein signals in tumor blood vessels and perivascular tumor cells (nuclear and cytoplasmic), as well as isolated tumor cells (Figure 1B). KANSL2 expression followed a gradient from the perivascular zone (described to be enriched for cancer cells with stem cell features) (15,39–41) towards the main body of the tumor (Figure 1C). In addition, enhanced KANSL2 expression in the tumor tissue was confirmed in a patient sample by analyzing the tumor area versus the contra-lateral healthy section from the same individual, observing low KANSL2 signal in a few isolated endothelial-like cells (Figure 1C).

Next, we assessed whether KANSL2 overexpression was correlated with tumor grade by analyzing *KANSL2* expression in 52 glioma tissue samples for which RNA expression profiling was available (24). We found no differences of *KANSL2* expression between high (IDH non-mutated) and low (IDH mutated) grade tumors (Figure 1D).

The KAT8/MOF/MYST acetyl-transferase complex, which targets lysine 16 in histone H4 (AcH4K16), was previously reported to be expressed in mouse ESCs and NPs (21,23). Along with the AcH4K16 marks, we determined the expression of KAT8 in GBM patient samples. *KAT8* mRNA levels ranged among tumor samples with no significant differences relative to normal cortex or the tumor grade (Figure 1E and F). At the protein level, KAT8 expression was detected in 43% of the samples (3/7) (Figure 1G and Table 1). Although KAT8 expression is variable, it seems to have a moderate correlation with AcH4K16 staining (Figure 1H and Table 1) (42,43).

The correlation of KANSL2 enrichment by qRT-PCR data, protein staining pattern in high-grade tumors (i.e. tumor grade III and IV vs normal cortex) and the presence of KANSL2 staining in areas related to the perivascular niches, suggested a potential role of KANSL2 in GBM, in particular, in GBSCs. Therefore, we tested the impact of *KANSL2* knockdown on the behavior of GBM cells lines.

KANSL2 depletion inhibits GBM-derived tumor growth

To gain further insight into the pathophysiological role of KANSL2 expression in GBM cells, we stably knocked-down *KANSL2* in human GBM U87MG, T98G and LN299 cell lines, using two independent shRNAs (referred hereto as KD-K2-1 and KD-K2-2), targeting the coding region and 3′ UTR of the KANSL2 mRNA, respectively. A non-targeting hairpin (NT) was used as control and knockdown efficiency was validated in KD-K2 cells (Figure 2A and B, and Supplementary Fig. S2A and B). KD-K2-U87MG cells or NT-U87MG cells were subcutaneously injected into each side flank of NOD*scid* mice and tumor growth rate was measured. Tumors derived from KD-K2-U87MG cells were significantly smaller compared to controls. The inhibitory effect on tumor growth was observed with both KANSL2 hairpins, minimizing the chances of off-target effects (Figure 2C–H). To confirm these results, we also evaluated KD-K2 cells derived from the human GBM cell line LN299 (KD-K2 LN299 cells), which displayed a similar inhibition of tumor growth (Supplementary Fig. S2). We also examined the ability of the KD-K2 cells to generate orthotopic tumors. For these studies, we inoculated cells into the forebrain of 7-week-old NOD*scid* mice. Consistently with the *in vitro* data and the xenotumors at the flank of the mice, depletion of KANSL2 reduced the ability to form tumors in the inoculated brains (Figure 2I). No changes were observed in the number of Ki-67-positive tumor cells (or in the necrosis percentage); however, the survival of the mice inoculated with KANSL2-depleted cells was significantly prolonged compared to mice injected with control glioma cells (Figure 2J and K).

KANSL2 expression is upregulated in GBSCs

Based upon the observation that KANSL2 is over-expressed in patient tumor samples and its expression is higher at the perivascular zones, we hypothesized that KANSL2 regulates *stemness* properties in GBM. To test this, we evaluated the impact of *KANSL2* depletion on *stemness*-associated markers. We observed reduced *POU5F1*, *NANOG* and *NESTIN* mRNA expression in adherent monolayers of KD-K2 cells (Figure 3A). GBM with reduced *POU5F1* expression would indicate decreased *stemness* with the concomitant reduction of *NESTIN* expression (8,12,13,44), suggesting a potential role of KANSL2 in GBM *stemness* properties. Accordingly, we observed an increased expression of the glial marker *GFAP* and the neural marker *TUBB3* in KD-K2 cells (Figure 3B), indicative of cell differentiation (8,12,13).

Previous reports described that KAT8 expression is essential for pluripotency in ESCs (21) and that KAT8 overexpression and H4K16 acetylation by KAT8 are hallmarks of embryogenesis and oncogenesis (42,43). We did not find differences in *KAT8* mRNA expression in human GBM samples; however, we observed overall higher staining in KAT8 and AcH4K16 in GBM tissues relative to normal tissue. The *KAT8* mRNA level reduction

observed in KD-K2 cells (Figure 3A) and a robust decrease in H4K16 acetylation could be explained by reduced KAT8 activity (21,42) (Supplementary Fig. S3B).

To further evaluate the potential link of KANSL2 and the GBM-associated *stemness* properties, we analyzed GBSCs sphere cultures (Figure 3C and D). In agreement with the fact that KANSL2 expression is up-regulated in GBM cells (Figure 1), we detected up-regulation of *KANSL2* expression in sphere cultures, along with increased expression of the stem cell markers *POU5F1, NANOG, SOX2* and *NESTIN,* (Figure 3E and F). Higher expression of *KAT8* mRNA was also noticed in these sphere cultures (Figure 3E and F). To further confirm that U87MG-derived spheres are indeed enriched in GBSCs, we compared their tumorigenic potential. U87MG spheres were more aggressive and lethal in intracranial xenograft assays compared to monolayers after brain inoculation of 10^5cells (Figures 3G). Furthermore, there was a significant delay in the animal survival rate that was comparable to the monolayer cultures, when the spheres culture cell number injected was reduce to 10^4 cells (Figure 3E).

To further confirm KANSL2 expression in GBSCs and acknowledging potential limitations in the cellular heterogeneity of commercial cell lines, we sorted U87MG cells and GBM patient-derived cells, named G03 and G08 (previously characterized as GBM cells enriched in GBSCs (25), with different levels of CD133 expression, an established GBSCs marker (Figure 3H–M) (25,30). Consistently, CD133 expression increased in U87MG spheres compared to monolayers, being KANSL2 expression significantly higher in CD133 positive subpopulation cells (CD133+) than in the CD133 negative subpopulation (CD133−), in all sorted GBSCs (Figures 3H–M). Additionally, increased expression of *NANOG* and *POU5F1* was detected in CD133+ cells concordantly with their increased self-renewal capacity (Supplementary Fig. S4). Altogether, these data indicate that KANSL2 is highly expressed in GBM cells with stem cell-like features suggesting a common up-regulation mechanism during culture conditions requiring *'stemness'* properties (Figure 3).

KANSL2 modulates self-renewal capacity of GBSCs

Next, we evaluated the potential role of KANSL2 in the regulation of self-renewal/differentiation properties of GBM cells. The serial neurosphere formation assay tests the self-renewal capacity of neuronal stem cells and brain tumor stem cells (29,45). Using neurosphere formation and the limiting dilution assays in suspension, we observed that the number of KD-K2-derived spheres was significantly lower compared to NT-derived spheres (Figure 4A, B and C). To confirm our results, clonogenic efficiency of KD-KANSL2 cells was measured using soft agar media under *stemness* conditions (30). Indeed, we found that KD-K2 cells have decreased clonogenicity compared to the control (Figure 4E and F). Furthermore, silencing of *KANSL2* in GBSCs enriched cells derived from sphere showed significant reduction of their growth in *in vitro* (Figure 4D) (30).

KANSL2 induces *POU5F1* expression in human glioblastoma cells

KANSL2 was overexpressed in tumor GBM samples and it is also enriched in GBSCs. Accordingly, silencing of KANSL2 reduces expression of embryonic stem factors *POU5F1* and *NANOG* and the self-renewal capacity of the cells (Figure 3 and 4). To confirm the

effect of KANSL2 in regulating stem cell factors, we transiently transfected the human GBM and HEK293 cells with either RFP- or the mouse version of Kansl2-RFP (pKansl2-RFP), which shares 95% identity with the human KANSL2 (Figure 5A–C). KANSL2 forced expression significantly increased *POU5F1* and *NANOG* promoter activities (Figure 5D and E). In agreement with the reporter assays, transient overexpression of KANSL2 increased the endogenous expression of *NANOG* and *POU5F1* in U87MG and in patient-derived G03 cells.

POU5F1 regulates KANSL2 expression

To further understand the molecular mechanism of KANSL2 function on *stemness*, we assessed the effect of POU5F1 on *KANSL2* expression. *POU5F1* expression was stably silenced with two independent shRNAs (referred as KD-POU5F1-1 and KD-POU5F1-2) (Figure 6A and B). As previously reported, downregulation of POU5F1 reduced the ability of human GBM cells to form gliomaspheres and decreased the expression of the neural progenitor *NESTIN* (Figure 6C and D) (12). In agreement with our *in silico* prediction, POU5F1 depletion led to lower *KANSL2* expression (Figure 6D and E). Altogether, these results suggest that POU5F1 and KANSL2 regulate each other in a positive feedback mechanism to control the *stemness* properties of GBM cells. Therefore, our work reveals a novel role for KANSL2 in the etiology and progression of GBM.

DISCUSSION

Glioblastoma is enriched in stem cell properties, which has been associated with the aggressiveness, therapy resistance and recurrence of this tumor type (1–5,46). Recently, GBM progression was associated to chromatin regulators and a core set of transcription factors that regulate cell fate commitment (47). CSCs, and particularly GBSCs, express many markers found in ESCs during normal development, which may drive tumor initiation and renewal. Using bioinformatic approaches, we identified genes involved in the regulation of SCs transcriptional networks (20), particularly in CSCs, which led us to identify *KANSL2* as a potential candidate.

In this report, we investigated the role of KANSL2 in GBM. We found that KANSL2 expression is increased in tumor cells regardless of glioma grade. Using loss-of-function approaches in GBM cell lines and GBSCs-enriched spheres, we determined that KANSL2 plays a tumorigenic role, promoting the clonogenicity and self-renewal capacity *in vitro*, and driving tumor growth *in vivo*, revealing a requirement for KANSL2 expression during GBM tumor growth.

The mechanisms governing KANSL2 expression in gliomas remain to be elucidated. However, we could determine that KANSL2 expression is dependent on POU5F1, and that POU5F1 is regulated by KANSL2 in human GBM cells, and both genes were upregulated under culture conditions requiring *stemness*. POU5F1 (as well as SOX2 and NANOG) (8) are essential pluripotency factors; is critical for GBM *stemness* and regulates gliomagenesis through several pathways (8,13,44,48). Our findings indicate that KANSL2 and POU5F1 are part of a common transcriptional network controlling *stemness* in this tumor type. In support of this notion, the gene expression profile of KANSL2 and POU5F1 are similar among

different human glioma tissues, GBSCs cells and embryonic cells, suggesting these two genes are either controlled by the same transcriptional regulatory program, functionally related and/or members of the same pathway or protein complex. Furthermore, utilizing the luciferase promoter-reporter assays, we revealed a regulatory link (either direct or indirect) between KANSL2 and POU5F1.

KANSL2, as a member of the NSL-complex (31–33) was linked to the control of cellular pluripotency, and to be required for global acetylation, including H4K16 acetylation in mouse ESCs, and for stem cell proliferation (21,23). Furthermore, modulation of KAT8 expression was reported during mouse ES cell differentiation into neuronal progenitors; while other KANSL proteins (i.e. KANSL1 and KANSL3) remained unaffected. Despite some discrepancies about the exact contribution of each KAT8-associated complex to *stemness* in mouse ESCs, their role in human ESCs, neural progenitors and/or during neurogenesis or cancer has not been previously investigated. (43). Similar to pluripotency factors, we observed that KANSL2 depletion led to a reduced expression of stem cell markers while increasing expression of lineage-specific markers such as *GFAP* and *TUBB3*, indicating that KANSL2 indeed could function as an inhibitor of cellular differentiation.

It has been proposed that overexpression of members of the KAT8-associated complex could drive tumor formation (42,43,49). Therefore, it is possible that KANSL2 overexpression in GBM and in particular in the GBSCs population affects the stoichiometry of these complexes resulting in a dysfunctional complex. Indeed, we were unable to select glioblastoma cells stably overexpressing KANSL2. However, transient KANSL2 over expression increased NANOG and POUF51 expression. We posit that KANSL2 expression levels and function could be influenced not only by its interaction partners but also by environmental inputs, having therefore an impact on the dynamic equilibrium of cell heritage identity. Additionally, we observed that KANSL2 depletion reduces AcH4K16, which could be explained by reduced catalytic activity of the NSL-complex or by reduced expression of KAT8. KANSL2 has been reported to interact with another member of the KAT8-associated complex, WDR5, a promoter of self-renewal in ES and tumor bladder cells (32,49), where POU5F1 expression level has been also proposed as a potential prognostic tumor marker (50).

The identification of novel genes involved in cancer progression through de-regulation of cell plasticity events that can regulate CSCs, and in particular GBSCs, is of clinical importance in GBM progression. It would be interesting to investigate whether KANSL2 plays a role as a regulator of stem capacity in other type of tumors where POU5F1 sustains *stemness*. Additionally, in order to expand the generality of our observations, it should be important to conduct future studies using more patient-derived cells, since they better represent the tumor biology and heterogeneity encountered daily in the clinic.

Altogether, our data indicate that *KANSL2* gene expression might be considered as a potential marker for GBM cells associated with stem cell properties and could be explored as a prognostic marker in this cancer type.

Supplementary Material

Refer to Web version on PubMed Central for supplementary material.

Acknowledgments

Grant Support: This work was supported by grants from Agencia Nacional de Promoción Científica y Técnica, Argentina, Consejo Nacional de Investigaciones Científicas y Técnicas, FOCEM-Mercosur (COF 03/11), NIH grants R01CA117907 and 5P30CA046934, and The Pew Latin American Fellows Program for the repatriation award. We also thank Bunge & Born Foundation and the Argentinian Instituto Nacional del Cáncer (INC) for financial support to Nazarena Ferreyra-Solari and Lucía Canedo, respectively.

We thank Ken Kobayashi (AGBT, FBMC-FCEN, IBBEA CONICET-UBA, Buenos Aires, Argentina) for critical reading, Marcelo Schultz (FLENI, Buenos Aires, Argentina) and IBioBA members (IBioBA-MPSM-CONICET, Buenos Aires, Argentina) for their technical assistance.

References

1. Louis DN, Ohgaki H, Wiestler OD, Cavenee WK, Burger PC, Jouvet A, et al. The 2007 WHO classification of tumours of the central nervous system. Acta Neuropathol. 2007; 114:97–109. [PubMed: 17618441]
2. Ostrom QT, Gittleman H, Farah P, Ondracek A, Chen Y, Wolinsky Y, et al. CBTRUS statistical report: Primary brain and central nervous system tumors diagnosed in the United States in 2006–2010. Neuro Oncol. 2013; 15(Suppl 2):ii1–56. [PubMed: 24137015]
3. Phillips HS, Kharbanda S, Chen R, Forrest WF, Soriano RH, Wu TD, et al. Molecular subclasses of high-grade glioma predict prognosis, delineate a pattern of disease progression, and resemble stages in neurogenesis. Cancer Cell. 2006; 9:157–73. [PubMed: 16530701]
4. Singh SK, Clarke ID, Terasaki M, Bonn VE, Hawkins C, Squire J, et al. Identification of a cancer stem cell in human brain tumors. Cancer Res. 2003; 63:5821–8. [PubMed: 14522905]
5. Zhou BB, Zhang H, Damelin M, Geles KG, Grindley JC, Dirks PB. Tumour-initiating cells: challenges and opportunities for anticancer drug discovery. Nat Rev Drug Discov. 2009; 8:806–23. [PubMed: 19794444]
6. Bao S, Wu Q, McLendon RE, Hao Y, Shi Q, Hjelmeland AB, et al. Glioma stem cells promote radioresistance by preferential activation of the DNA damage response. Nature. 2006; 444:756–60. [PubMed: 17051156]
7. Clement V, Sanchez P, de Tribolet N, Radovanovic I, Ruiz i Altaba A. HEDGEHOG-GLI1 signaling regulates human glioma growth, cancer stem cell self-renewal, and tumorigenicity. Curr Biol. 2007; 17:165–72. [PubMed: 17196391]
8. Ikushima H, Todo T, Ino Y, Takahashi M, Miyazawa K, Miyazono K. Autocrine TGF-beta signaling maintains tumorigenicity of glioma-initiating cells through Sry-related HMG-box factors. Cell Stem Cell. 2009; 5:504–14. [PubMed: 19896441]
9. Penuelas S, Anido J, Prieto-Sanchez RM, Folch G, Barba I, Cuartas I, et al. TGF-beta increases glioma-initiating cell self-renewal through the induction of LIF in human glioblastoma. Cancer Cell. 2009; 15:315–27. [PubMed: 19345330]
10. Safa AR, Saadatzadeh MR, Cohen-Gadol AA, Pollok KE, Bijangi-Vishehsaraei K. Glioblastoma stem cells (GSCs) epigenetic plasticity and interconversion between differentiated non-GSCs and GSCs. Genes Dis. 2015; 2:152–63. [PubMed: 26137500]
11. Cheng L, Sung MT, Cossu-Rocca P, Jones TD, MacLennan GT, De Jong J, et al. OCT4: biological functions and clinical applications as a marker of germ cell neoplasia. J Pathol. 2007; 211:1–9. [PubMed: 17117392]
12. Du Z, Jia D, Liu S, Wang F, Li G, Zhang Y, et al. Oct4 is expressed in human gliomas and promotes colony formation in glioma cells. Glia. 2009; 57:724–33. [PubMed: 18985733]
13. Ikushima H, Todo T, Ino Y, Takahashi M, Saito N, Miyazawa K, et al. Glioma-initiating cells retain their tumorigenicity through integration of the Sox axis and Oct4 protein. J Biol Chem. 2011; 286:41434–41. [PubMed: 21987575]

14. Nichols J, Zevnik B, Anastassiadis K, Niwa H, Klewe-Nebenius D, Chambers I, et al. Formation of pluripotent stem cells in the mammalian embryo depends on the POU transcription factor Oct4. Cell. 1998; 95:379–91. [PubMed: 9814708]
15. Gilbertson RJ, Rich JN. Making a tumour's bed: glioblastoma stem cells and the vascular niche. Nat Rev Cancer. 2007; 7:733–6. [PubMed: 17882276]
16. Grskovic M, Chaivorapol C, Gaspar-Maia A, Li H, Ramalho-Santos M. Systematic identification of cis-regulatory sequences active in mouse and human embryonic stem cells. PLoS Genet. 2007; 3:e145. [PubMed: 17784790]
17. Kim J, Chu J, Shen X, Wang J, Orkin SH. An extended transcriptional network for pluripotency of embryonic stem cells. Cell. 2008; 132:1049–61. [PubMed: 18358816]
18. Sun Y, Li H, Liu Y, Mattson MP, Rao MS, Zhan M. Evolutionarily conserved transcriptional co-expression guiding embryonic stem cell differentiation. PLoS One. 2008; 3:e3406. [PubMed: 18923680]
19. Sun Y, Li H, Liu Y, Shin S, Mattson MP, Rao MS, et al. Cross-species transcriptional profiles establish a functional portrait of embryonic stem cells. Genomics. 2007; 89:22–35. [PubMed: 17055697]
20. Rohr CO, Parra RG, Yankilevich P, Perez-Castro C. INSECT: IN-silico SEarch for Co-occurring Transcription factors. Bioinformatics. 2013; 29:2852–8. [PubMed: 24008418]
21. Chelmicki T, Dundar F, Turley MJ, Khanam T, Aktas T, Ramirez F, et al. MOF-associated complexes ensure stem cell identity and Xist repression. Elife. 2014; 3:e02024. [PubMed: 24842875]
22. Feller C, Prestel M, Hartmann H, Straub T, Soding J, Becker PB. The MOF-containing NSL complex associates globally with housekeeping genes, but activates only a defined subset. Nucleic Acids Res. 2012; 40:1509–22. [PubMed: 22039099]
23. Ravens S, Fournier M, Ye T, Stierle M, Dembele D, Chavant V, et al. Mof-associated complexes have overlapping and unique roles in regulating pluripotency in embryonic stem cells and during differentiation. Elife. 2014; 3:e02104.
24. Ferrer-Luna R, Mata M, Nunez L, Calvar J, Dasi F, Arias E, et al. Loss of heterozygosity at 1p-19q induces a global change in oligodendroglial tumor gene expression. J Neurooncol. 2009; 95:343–54. [PubMed: 19597701]
25. Videla Richardson GA, Garcia CP, Roisman A, Slavutsky I, Fernandez Espinosa DD, Romorini L, et al. Specific Preferences in Lineage Choice and Phenotypic Plasticity of Glioma Stem Cells Under BMP4 and Noggin Influence. Brain Pathol. 2015; 26:43–61. [PubMed: 25808628]
26. Mandal P, Chauhan S, Tomar RS. H3 clipping activity of glutamate dehydrogenase is regulated by stefin B and chromatin structure. FEBS J. 2014; 281:5292–308. [PubMed: 25263734]
27. Sanders YY, Liu H, Zhang X, Hecker L, Bernard K, Desai L, et al. Histone modifications in senescence-associated resistance to apoptosis by oxidative stress. Redox Biol. 2013; 1:8–16. [PubMed: 24024133]
28. Livak KJ, Schmittgen TD. Analysis of relative gene expression data using real-time quantitative PCR and the 2(−Delta Delta C(T)) Method. Methods. 2001; 25:402–8. [PubMed: 11846609]
29. Hu Y, Smyth GK. ELDA: extreme limiting dilution analysis for comparing depleted and enriched populations in stem cell and other assays. J Immunol Methods. 2009; 347:70–8. [PubMed: 19567251]
30. Brescia P, Ortensi B, Fornasari L, Levi D, Broggi G, Pelicci G. CD133 is essential for glioblastoma stem cell maintenance. Stem Cells. 2013; 31:857–69. [PubMed: 23307586]
31. Cai Y, Jin J, Swanson SK, Cole MD, Choi SH, Florens L, et al. Subunit composition and substrate specificity of a MOF-containing histone acetyltransferase distinct from the male-specific lethal (MSL) complex. J Biol Chem. 2010; 285:4268–72. [PubMed: 20018852]
32. Dias J, Van Nguyen N, Georgiev P, Gaub A, Brettschneider J, Cusack S, et al. Structural analysis of the KANSL1/WDR5/KANSL2 complex reveals that WDR5 is required for efficient assembly and chromatin targeting of the NSL complex. Genes Dev. 2014; 28:929–42. [PubMed: 24788516]
33. Mendjan S, Taipale M, Kind J, Holz H, Gebhardt P, Schelder M, et al. Nuclear pore components are involved in the transcriptional regulation of dosage compensation in Drosophila. Mol Cell. 2006; 21:811–23. [PubMed: 16543150]

34. Raja SJ, Charapitsa I, Conrad T, Vaquerizas JM, Gebhardt P, Holz H, et al. The nonspecific lethal complex is a transcriptional regulator in Drosophila. Mol Cell. 2010; 38:827–41. [PubMed: 20620954]
35. Pal R, Ravindran G. Assessment of pluripotency and multilineage differentiation potential of NTERA-2 cells as a model for studying human embryonic stem cells. Cell Prolif. 2006; 39:585–98. [PubMed: 17109641]
36. Przyborski SA, Christie VB, Hayman MW, Stewart R, Horrocks GM. Human embryonal carcinoma stem cells: models of embryonic development in humans. Stem Cells Dev. 2004; 13:400–8. [PubMed: 15345134]
37. Goffart N, Kroonen J, Rogister B. Glioblastoma-initiating cells: relationship with neural stem cells and the micro-environment. Cancers (Basel). 2013; 5:1049–71. [PubMed: 24202333]
38. Lee da Y, Gianino SM, Gutmann DH. Innate neural stem cell heterogeneity determines the patterning of glioma formation in children. Cancer Cell. 2012; 22:131–8. [PubMed: 22789544]
39. Bao S, Wu Q, Sathornsumetee S, Hao Y, Li Z, Hjelmeland AB, et al. Stem cell-like glioma cells promote tumor angiogenesis through vascular endothelial growth factor. Cancer Res. 2006; 66:7843–8. [PubMed: 16912155]
40. Calabrese C, Poppleton H, Kocak M, Hogg TL, Fuller C, Hamner B, et al. A perivascular niche for brain tumor stem cells. Cancer Cell. 2007; 11:69–82. [PubMed: 17222791]
41. Li Z, Bao S, Wu Q, Wang H, Eyler C, Sathornsumetee S, et al. Hypoxia-inducible factors regulate tumorigenic capacity of glioma stem cells. Cancer Cell. 2009; 15:501–13. [PubMed: 19477429]
42. Gupta A, Guerin-Peyrou TG, Sharma GG, Park C, Agarwal M, Ganju RK, et al. The mammalian ortholog of Drosophila MOF that acetylates histone H4 lysine 16 is essential for embryogenesis and oncogenesis. Mol Cell Biol. 2008; 28:397–409. [PubMed: 17967868]
43. Liu Y, Long Y, Xing Z, Zhang D. C-Jun recruits the NSL complex to regulate its target gene expression by modulating H4K16 acetylation and promoting the release of the repressive NuRD complex. Oncotarget. 2015; 6:14497–506. [PubMed: 25971333]
44. Holmberg J, He X, Peredo I, Orrego A, Hesselager G, Ericsson C, et al. Activation of neural and pluripotent stem cell signatures correlates with increased malignancy in human glioma. PLoS One. 2011; 6:e18454. [PubMed: 21483788]
45. Laks DR, Masterman-Smith M, Visnyei K, Angenieux B, Orozco NM, Foran I, et al. Neurosphere formation is an independent predictor of clinical outcome in malignant glioma. Stem Cells. 2009; 27:980–7. [PubMed: 19353526]
46. Chen R, Nishimura MC, Bumbaca SM, Kharbanda S, Forrest WF, Kasman IM, et al. A hierarchy of self-renewing tumor-initiating cell types in glioblastoma. Cancer Cell. 2010; 17:362–75. [PubMed: 20385361]
47. Kozono D, Li J, Nitta M, Sampetrean O, Gonda D, Kushwaha DS, et al. Dynamic epigenetic regulation of glioblastoma tumorigenicity through LSD1 modulation of MYC expression. Proc Natl Acad Sci U S A. 2015; 112:E4055–64. [PubMed: 26159421]
48. Morfouace M, Lalier L, Oliver L, Cheray M, Pecqueur C, Cartron PF, et al. Control of glioma cell death and differentiation by PKM2-Oct4 interaction. Cell Death Dis. 2014; 5:e1036. [PubMed: 24481450]
49. Chen X, Xie W, Gu P, Cai Q, Wang B, Xie Y, et al. Upregulated WDR5 promotes proliferation, self-renewal and chemoresistance in bladder cancer via mediating H3K4 trimethylation. Sci Rep. 2015; 5:8293. [PubMed: 25656485]
50. Hatefi N, Nouraee N, Parvin M, Ziaee SA, Mowla SJ. Evaluating the expression of oct4 as a prognostic tumor marker in bladder cancer. Iran J Basic Med Sci. 2012; 15:1154–61. [PubMed: 23653844]

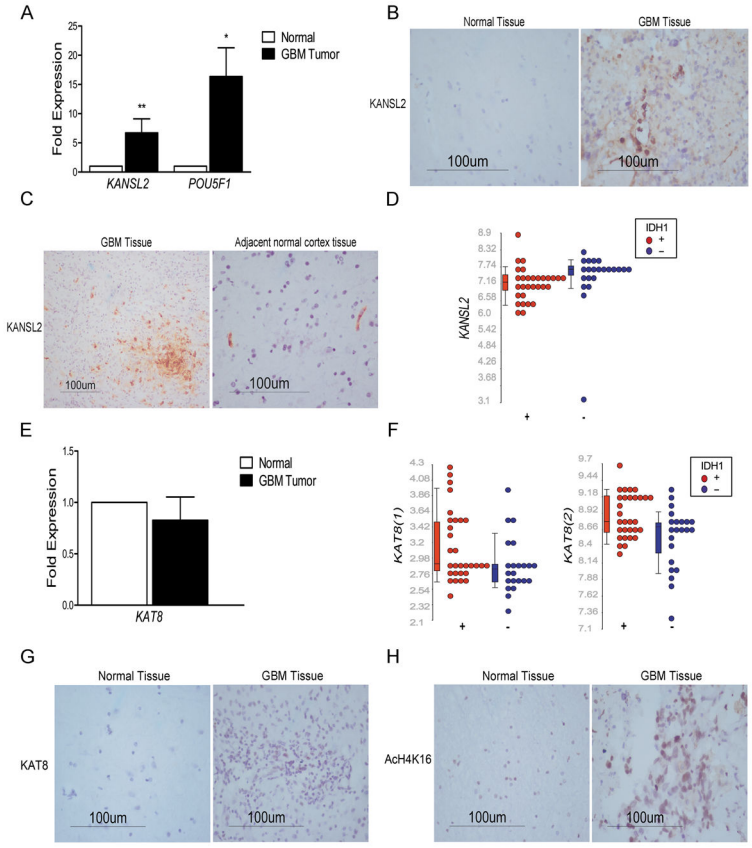

Figure 1.

KANSL2, KAT8 and AcH4K16 expression pattern in human GBM samples. A, qRT-PCR analysis of *KANSL2* and *POU5F1* in human GBM tumors (n=8) and a control (human cortex). Values were normalized to those corresponding to normal tissue. Results are expressed as mean ± SEM. B, Normal tissue samples have no detectable KANSL2 signals; GBM have moderate to intense KANSL2 expression (400x) and is mainly confined to tumor blood vessels and perivascular tumor cells. Few isolated cells with strong KANSL2 staining were also observed. C, KANSL2 staining gradient from the perivascular zone toward the main body of the tumor is shown (200x). KANSL2 positive signal in isolated endothelial-like cells was found at the adjacent normal cortex tissue of this sample (400x). D, Dot plot of *KANSL2* expression showing the distribution of probeset intensities across all 52 glioma samples (Affymetrix HU133plus2.0 genechip). *KANSL2* expression did not correlate with high (IDH1-) nor low (IDH1+) tumor grade (Supplementary Table S1). E, qRT-PCR analysis of *KAT8* in human GBM tumors (n=8) and a control (human cortex). F, Dot plot of *KAT8* expression across all 52 glioma samples, as showing in D. None of *KAT8 (1) and KAT8 (2)*, correlated with high (IDH1-) nor low (IDH1+) glioma grade. G and H, Representative images of KAT8 and AcH4K16 IHQ staining are shown. Normal tissue samples have negative or weak KAT8 or AcH4K16 signals. GBM samples have a variable mild expression of KAT8 and AcH4K16 in (400x).

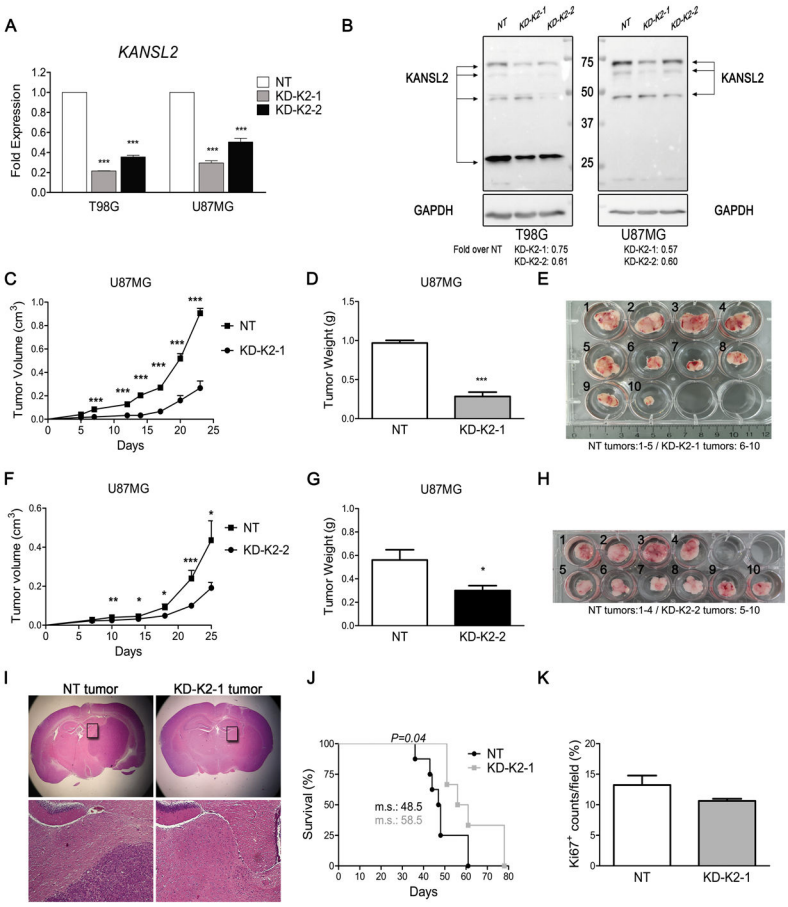

Figure 2.

KANSL2 knockdown inhibits tumor growth in a xenograft model. A, qRT-PCR analysis of KD-K2-1 and KD-K2-2 U87MG and T98G cells showing significantly suppressed *KANSL2* mRNA levels compared to NT (U87MG KD-K2-1, 70.52% ± 2.19 and KD-K2-2, 49.62% ± 3.7 knockdown and T98G KD-K2-1, 78.6% ± 0.17 and KD-K2-2, 64.57% ± 1.60 knockdown). Results are expressed as mean ± SEM from three independent measurements. *, P≤0.005; ***, P≤0.0005. B, western blot analysis showing a KANSL2 protein level decreased. Average fold decrease of KANSL2 protein accumulation is shown below each cell line. C–H, subcutaneously injected NOD*scid* mice with 2×10^6 U87MG cells stably expressing control shRNA (NT) or KANSL2 shRNA (KD-K2-1 or KD-K2-2). C and F, Average tumor volume ± SEM is plotted against time (in days). *P≤0.05, **P≤0.005, ***P≤0.0005. D and G, tumor weight at between 3–4 weeks after injection. *P≤0.05, ***P≤0.0005. E and H, Representative photographs of tumors excised from mice. I, images of H&E staining and coronal sections from representative mice brains dissected at day 36–44 after intracerebral injected with 10^5 NT (n=3) and KD-K2-1 (n=3) cells are shown. J, survival of mice was evaluated by Kaplan-Meier analysis; p values were calculated by the log-rank test (NT, n=6; KD-K2-1, n =4). K, Quantitation of Ki67-positive cells in brain sections in end point of indicated mice from J. Results are expressed as mean ± SEM.

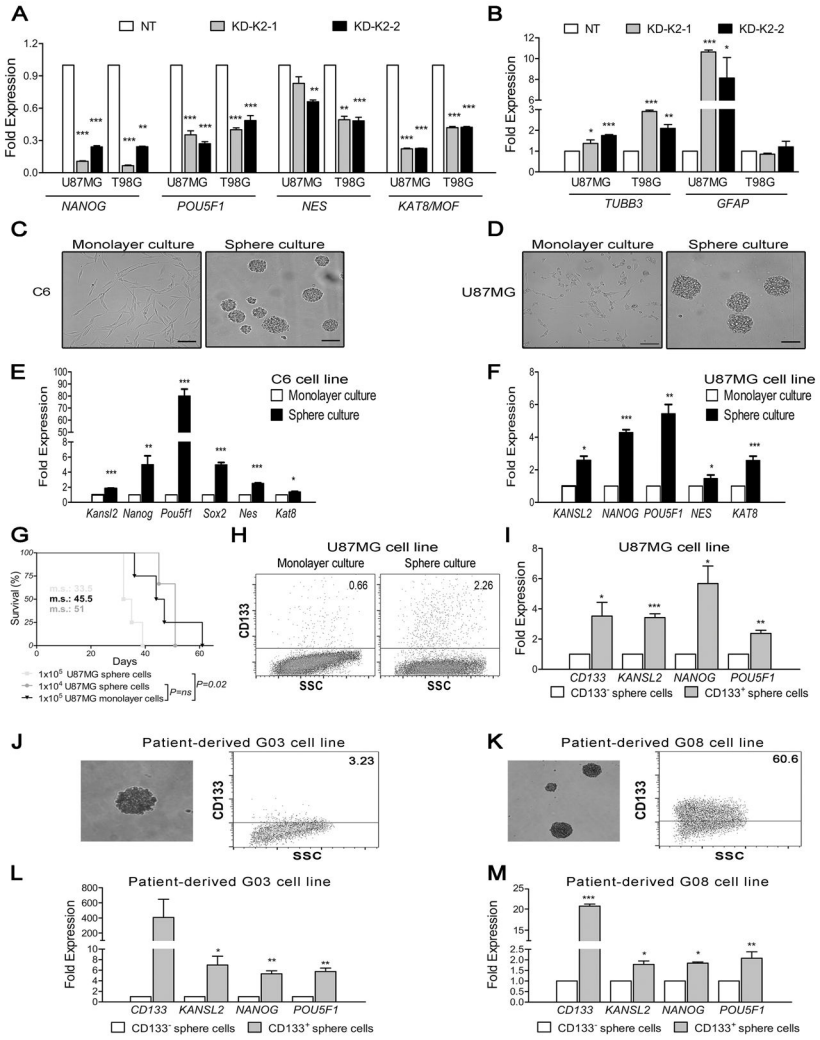

Figure 3.

KANSL2 expression is upregulated in GBSC enriched-culture. A and B, qRT-PCR analysis of KD-K2-1 and KD-K2-2 cells showing significantly decreased expression of *NANOG, POU5F1, NESTIN* and *KAT8* and an increased expression of *GFAP* and *TUBB3* compared to NT cells. C and D, images of rat C6 and human U87MG GBM cells grown as monolayers or neurospheres. Scale bars: 100 μm. E and F, C6 and U87MG cells grown as spheres enriched in GBSC showing an increased expression of SC markers (*NANOG*, *POU5F1, SOX2, NESTIN, KAT8*) and *KANSL2*, quantified by qRT-PCR. Gene expression levels in sphere were normalized to their expression in monolayer cultures. G, survival percentage of mice evaluated by Kaplan-Meier analysis; p values were calculated by the log-rank test, showing an enhanced aggressive and lethal potency in intracranial xenograft assays compared to monolayers. H, FACS analysis of CD133 expression in U87MG monolayer vs spheres cultures. U87MG spheres are enriched in CD133 expression. I, qRT-PCR analysis of CD133, *KANSL2*, *NANOG* and *POUF51* in U87MG CD133+ and CD133- cells subpopulations. KANSL2 expression is enhanced in CD133 + cells together with the stem cell markers. J and K, phase-contrast microscopy images, FACS analysis and sorting for

CD133 of G03 and G08 patient-derived cells. L and M, qRT-PCR analysis of gene expression in patient-derived CD133+ and CD133- cells subpopulations. KANSL2 expression is enhanced in CD133 + cells together with the SCs markers. Results are expressed as mean ± SEM. **, $P \leq 0.005$; ***, $P \leq 0.0005$.

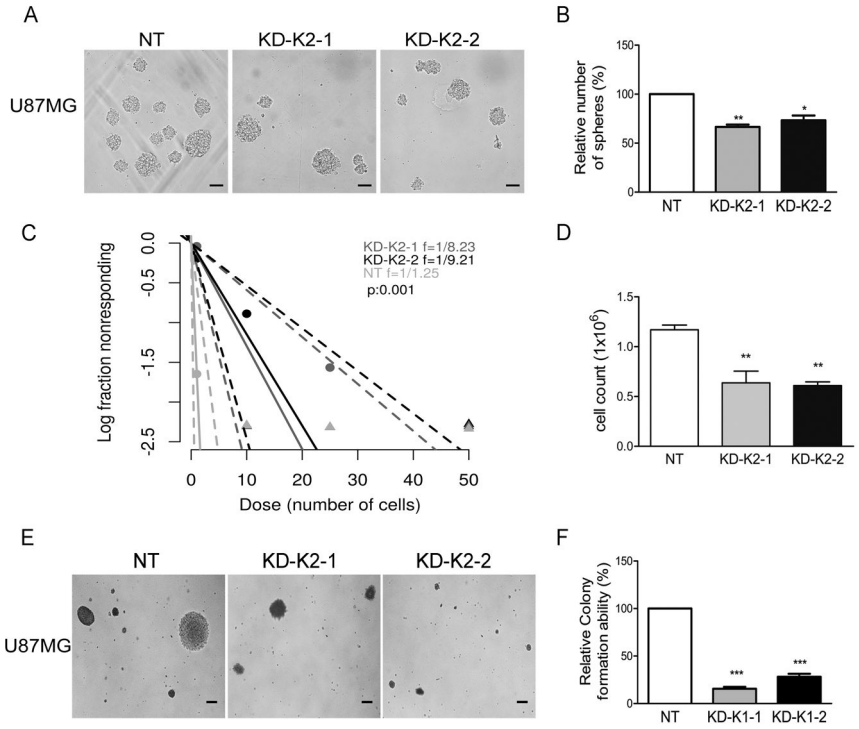

Figure 4.

KANSL2 modulates self-renewal capacity of GBSCs cells. A, phase-contrast microscopy images of NT and *KANSL2* knockdown KD-K2-1 and KD-K2-2 U87MG-spheres after 7 days. Scale bar: 100μm. B, number of GBSC, KD-K2-1- and KD-K2-2-derived spheres expressed as percentage of sphere relative to NT ± SEM. A representative experiment from three independent experiments with similar results is shown. *, P≤0.05; **, P≤0.005. C, stem cell frequency was calculated using online Extreme Limiting Dilutions Assay (ELDA) analysis program. Significant differences in stem cell frequencies was determined between NT (1/2.25) and KD-K2-1 (1/8.23) or KD-K2-2 (1/9.21) cells. D, relative cell proliferation assay by direct cell counting of dissociated cells. KD-K2-1 and KD-K2-2 showing significantly reduced proliferation activity. **, P ≤ 0.005. Results are expressed as mean ± SEM of a representative experiment of three experiments. E, representative images of colonies growing in soft agar assay in NSC media (5 × magnification). Scale bar: 100 μm. F, colony number quantification of the soft agar assays presented in D. Results are expressed as percentage of colonies relative to NT ± SEM. ***, P≤0.0005.

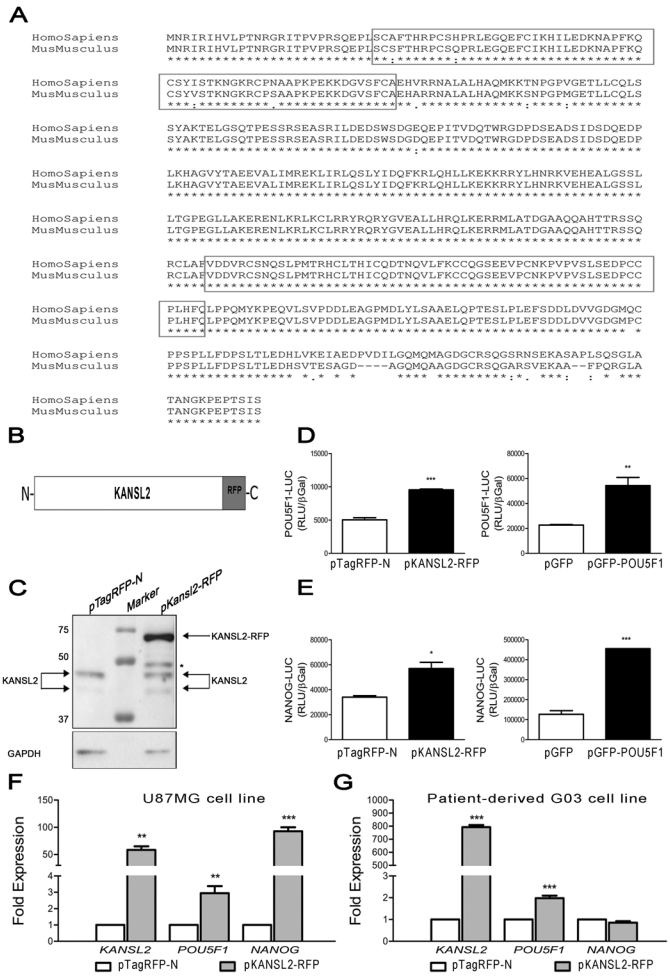

Figure 5.

Enhanced KANSL2 expression increases POU5F1 expression in GBM cells. A, Amino acid sequences alignment of hKANSL2 and mKANSL2 showing 95% shared identity. Predicted DNA binding domains are shown. B, schematic representation of KANSL2-RFP constructs. C, Western blot analysis from HEK293 cells transfected to expressed RFP-tagged KANSL2 and immunoblotting for KANSL2. * Band probably correspond a partial proteolytic product. D and E, POU5F1 and NANOG promoter-driven Luciferase assay in HEK293 cells transfected with either RFP or KANSL2-RFP showing induced POU5F1 and NANOG activity. As control, cells were either transfected with GFP or pGFP-OCT4 (pGFP-POU5F1). F and G, qRT-PCR analysis of *KANSL2*, *POU5F1* and *NANOG* in U87MG cells or patient-derivate G03 cells transfected with RFP or KANSL2-RFP expressing cells, showing induced *POU5F1* and/or *NANOG* endogenous expression in KANSL2-RFP cells, respectively. Data shown are the mean ± SEM. of at least two independent experiments. ***, P≤0.0005, **, P≤0.005, *, P≤0.05.

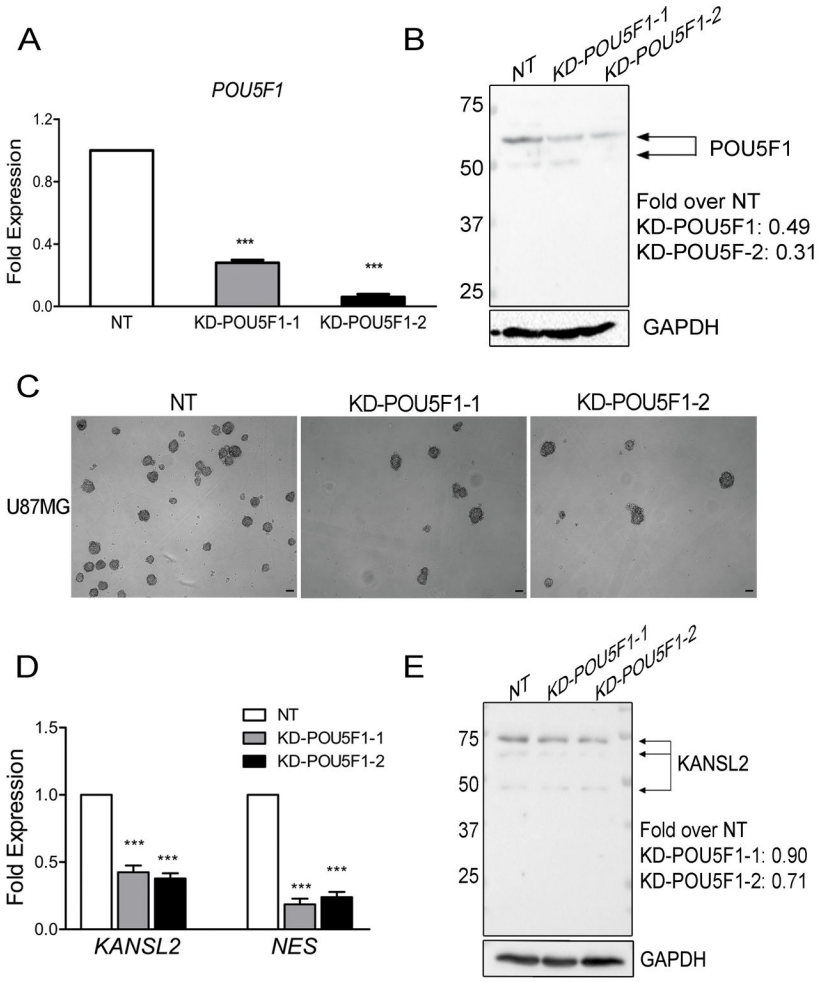

Figure 6.

POU5F1 regulates KANSL2 expression. A, *POU5F1* qRT-PCR analysis showing U87MG KD-POU5F1-1 and KD-POU5F1-2 cells have significantly decreased *POU5F1* expression relative to U87MG NT. B, Western blot analysis of POU5F1 expression showing the knockdown efficiency at the protein level. Fold-decrease expression is shown for each hairpin. C, images of NT, KD-POU5F1-1 and KD-POU5F1-2 U87MG-sphere cultured in NSC medium for 7 days. Knockdown of *POU5F1* in U87MG cells decreased the number of glioma spheres. Scale bar: 100 μm. D and E, qRT-PCR and Western blot analysis showing significantly reduced expression of *KANSL2* and *NESTIN* in U87MG KD-POU5F1-1 and KD-POU5F1-2 cells. Results are expressed as mean ± SEM. ***, P≤0.0005.

Table 1

Clinical, pathological and protein expression in glioma and normal biopsy.

		Age (years)	Localization	Histological Diagnosis	WHO grade	KANSL2	MOF	H4K16
Patients								
	1	27	Frontal	Anaplastic Oligodendroglioma	III	+ (6.32)	−	−
	2	71	midbrain	Anaplastic Oligoastrocytoma	III	+ (1.89)	−	−
	3	48	Temporal	Anaplastic Oligoastrocytoma	III	+++ (35.26)	−	+++
	4	29	Temporal	Anaplastic Oligoastrocytoma	III	+ (10.34)	+	+/−
	5	59	Fronto-temporal	Glioblastoma	IV	++ (16.50)	+++	+++
	6	52	Temporal	Glioblastoma	IV	+ (14.10)	+	+
	7	62	Parietal	Glioblastoma	IV	+++ (10.81)	−	−
Normal Tissues								
	Autopsy 1	43	Frontal cortex	Normal		−	−	+/−
	Autopsy 2	74	Frontal cortex	Normal		−	−	−
	Autopsy 3	57	Frontal cortex	Normal		−	−	+/−
	Autopsy 4	60	Frontal cortex	Normal		−	−	−
	Autopsy 5	27	Frontal cortex	Normal		−	−	+
	Autopsy 6	43	Frontal cortex	Normal		−	−	+/−
	Autopsy 7	41	Frontal cortex	Normal		−	−	+/−
	Patient 2*	71	Frontal cortex	Normal		+/−	−	−

+++: high, ++: medium, +:low, +/−:isolated and low, −: negative